HOW SAFE ARE RESPONSE CONTROLLED STRUCTURES? LIMIT STATES OF DAMPERS AND PROBABILISTIC RISK

Kit MIYAMOTO*, CEO and Principal, Miyamoto International Inc.
1450 Halyard Drive, Suite One, West Sacramento, CA, 95691, USA
Email:kmiyamoto@miyamotointernational.com
Amir GILANI, Structural Specialist, Engineering Div. Miyamoto International Inc.
1450 Halyard Drive, Suite One, West Sacramento, CA, 95691, USA
Email:agilani@miyamotointernational.com
Akira WADA, Professor, Tokyo Institute of Technology
4259 Nagatsuta-cho, Midori-ku, Yokohama, 226-8502,, JAPAN
Email: wada@serc.titech.ac.jp

Keywords: Viscous dampers, Limit states, Nonlinear analysis, Collapse margin ratio, Collapse probability

Summary
Viscous Dampers provide a reliable and convenient method of dissipating the seismic energies and thus protect structural and non structural components. Structures properly designed are expected to have superior performance under code level intensities (500 and 2500 year return events). Dampers are sized for the 2500 year event using force, velocity, and displacements obtained from analysis. Typically, a factor of safety of 1.0 (new) or 1.3 (retrofit) is used to protect the units from overload. The importance and adequacy of these factors of safety has not been established. Viscous dampers undergo fundamental constitutive changes after their capacity is reached: converting to a stiff steel brace upon reaching stroke limit, and failing after the force threshold. Analytical investigations were conducted to assess the response of damped structures to very large seismic events. An advanced mathematical model of viscous dampers, incorporating limit states, was developed. The post-limit response was correlated to laboratory tests of dampers reaching both stroke and capacity limits. Incremental dynamic analyses were conducted to assess the probability of collapse for the current design practice.

1. Introduction
Viscous dampers were originally developed as shock absorbers for the defense and aerospace industries. Currently, they are being used widely for seismic protection of new and retrofit of vulnerable structures. During seismic events, the input energy is converted to heat energy and is thus dissipated. Subsequent to installation, the dampers require minimal maintenance. Dampers have been shown to possess stable and dependable properties for design earthquakes. Figure 1 depicts the application of dampers to a new building in California[1)]. No comprehensive investigation has been under-taken to investigate limit state of viscous dampers and to characterize the effects of such limit states on the building response. Such examination is the subject of this paper. Sample results from an ongoing research currently underway to evaluate the performance of steel moment frames with dampers will be presented.

2. Modeling of Viscous Dampers

2.2 Overview
Viscous dampers consist of a cylinder and a stainless steel piston. The cylinder is filled with incompressible silicone fluid. The damper is activated by the flow of silicone fluid between chambers at opposite ends of the unit, through small orifices. Figure 2 shows a damper cross section.

Fig.1: Viscous dampers used for design of a new building in California

2.2 Maxwell Model

In most applications, the dampers are modeled as simple Maxwell model of Figure 3. The viscous damper itself is modeled as a dashpot in series with the elastic driver brace member. Such model is adequate for most design applications, but is not sufficiently refined for collapse evaluation. In particular, force and displacement limit states of the damper are unaccounted.

Fig.2: Viscous damper cross section

Fig.3: Maxwell model

2.3 Damper Limit States

The limit states of viscous dampers are governed by the following components:

- When the piston motion reaches its available stroke, the damper bottoms out. This is the stroke limit and results in transition from viscous damper to a steel brace with stiffness equal to that of the cylinder wall.
- Once the piston undercut fractures in tension or the driver brace reaches its compression capacity, the damper fails and is no longer effective.
- The orifice limit state is reached at high velocities. However, this limit state does not significantly alter the damper response. Such limit state results in change in the damper exponent (α).

2.4 Refined Model for Viscous Dampers

Figure 4 presents the proposed refined model for viscous dampers. This model is developed to incorporate the pertinent limit states and consists of five components. The refined model consists of the following components.

- The driver brace used to attach the damper to the gusset plates at the beam-to-column connection is modeled as a nonlinear spring.
- The piston rod (including the piston undercut) is modeled as a nonlinear spring. The piston undercut is the machined down section between the end of the piston and the start of the piston male threaded part. In tension, the undercut section of the piston can yield and then fracture. The undercut area is approximately 80% of the full piston area. The piston ultimate strength is only 10% above yield. Hence, fracture follows yielding rapidly; see Figure 5.
- Dashpot is used to model the viscous component.
- Gap element and linear springs are used to model the limit state when the piston retraction equals the stroke. The elastic stiffness depends on the damper construction and its cylinder properties.

- Hook elements and linear springs are used to model the limit state when the piston extension reaches the damper stroke. The stiffness is the same as above for the gap element.

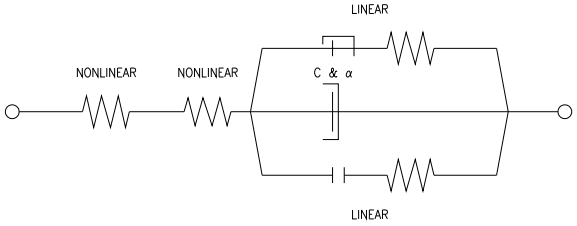

Fig.4: Refined model for viscous dampers

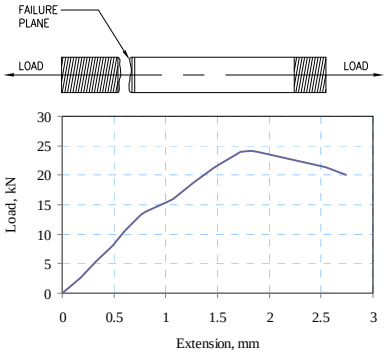

Fig.5: Piston undercut and test data

3. Analytical Simulations

To illustrate the response of the refined model and illustrate its capability to capture all the limit states, simulations were conducted. The damper was modeled in program OpenSees using the refined model[2]. All analysis was conducted using a sinusoidal displacement input function. The damper used in simulation is the 700-kN unit and has a constitutive relation (force in kN and velocity in mm/sec) of Eq. 1

$$F = 88\,\mathrm{sgn}(v)|v|^{0.3} \tag{1}$$

3.1 Force Limit State of Piston Fracture

This simulation was conducted to investigate the damper response for the limit state of piston undercut fracture. The stroke was artificially set to be large enough to ensure that the damper did not bottom out in compression. The response is shown in Figure 6. Note that the force transmitted by the cylinder walls is zero since the damper has not bottomed out. Once the piston undercut reaches its tensile capacity, the damper element is automatically removed from the simulation and the forces drop to zero.

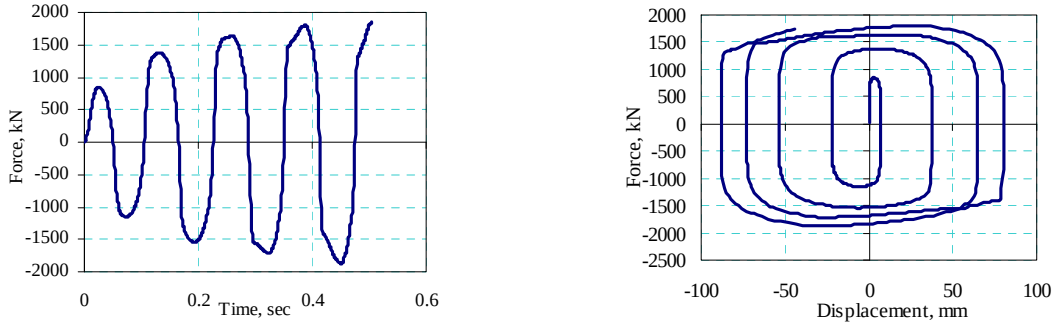

Fig.6: Force limit state simulation: force in the damper and unit hysteresis

3.2 Stroke Limit States

This simulation was conducted to investigate the damper response for the limit state when the stroke limit in extension and retraction are reached. The undercut tensile piston and driver brace compressive capacity were artificially set to be large enough for these members to remain elastic. The response is shown in Figure 7. Note that the force transmitted by the cylinder walls is non-zero once the stoke limit in either tension or compression is reached. The total force transmitted by the damper is the sum of displacement-proportional elastic force in the cylinder wall and velocity-proportional force in the viscous component (Kelvin model). Once the stoke limit is reached, the velocity drops to zero and thus the force in the

viscous element is zero. In structural applications, this will tend to translate to increased lateral stiffness and decreased effective damping ratio.

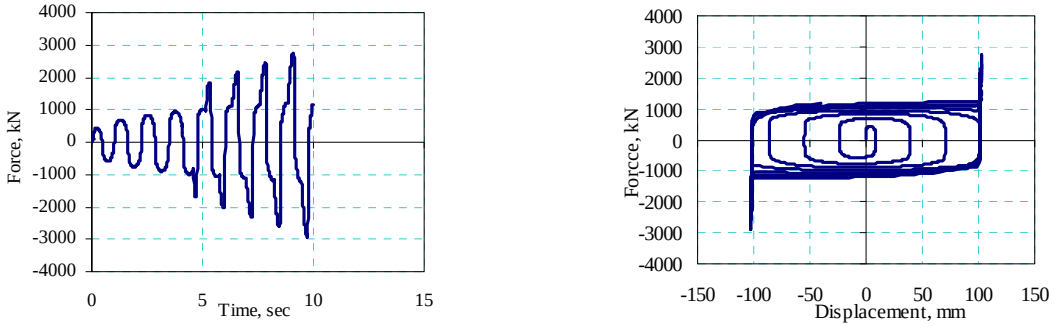

Fig.7: Displacement limit state simulation: force in the damper and unit hysteresis

3.3 Compound Limit State

The stroke limit is reached first. If the loading is increased, then the driver will buckle in compression or the undercut will yield and fracture in tension. This simulation was conducted to investigate the damper response for the limit state of piston fracture following the bottoming out of damper at full extension. The response is shown in Figure 8. At 4.5 sec in the response, the piston extension reaches the stroke limit and the damper bottoms out. At this point, velocity is zero and thus the force in the viscous element drops to zero. The damper acts as an elastic brace. The undercut yields but does not fracture. Loading is then reversed. This results in the disengagement of cylinder walls, and re-loading of the viscous component. At 5.3 sec, piston bottoms out again. The damper again becomes an elastic brace. Loading is increased further resulting in fracture of undercut. The entire damper is now ineffective and removed.

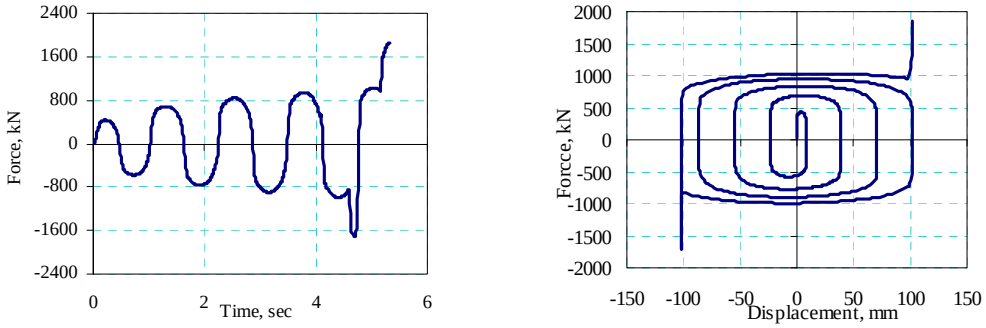

Fig.8: Compound limit state simulation: force in the damper and unit hysteresis

4. Correlation With Test Results

Experimental data from a damper was used to assess the accuracy of the refined mathematical model of dampers[3]. This damper was laboratory tested and was subjected to large velocity and displacement pulses in succession and experienced several of its limit states. This damper had a nominal capacity of 2000 kN at a velocity of 330 mm/sec. It had a stroke of 140 mm. Its constitutive relation (force in kN and velocity in mm/sec) is presented in Eq 2.

$$F = 195\,\mathrm{sgn}(v)|v|^{0.4} \tag{2}$$

The damper was placed in the test rig and subject to a displacement loading history. The unit was placed with its piston extended to within 10 mm of the stroke limit prior to start of the displacement cycles. At 4.3 sec, the unit was pulled in tension with a large velocity pulse. The motion was reversed just prior to reaching the stroke limit. At 4.61 sec, the damper bottoms

out in compression, resulting in sharp increase in the measured force. This is followed by tensile yielding. Finally at 4.68 sec, fracture occurs and the damper load drops to zero. After this time, no force can be transferred by the damper. The experimental data are presented as solid lines in Figure 9. The dashed lines in these figures represent the results obtain from simulation using the refined damper element. Good correlation is obtained between the experimental data and analytical simulations. The analytical model was able to capture the bottoming of the damper and tensile fracture accurately.

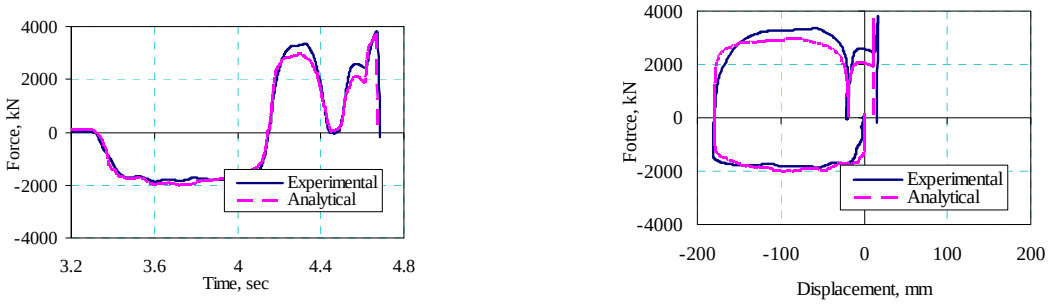

Fig.9: Correlation with experimental data: damper force and hysteresis loops

5. Nonlinear Analysis Methodology

The input histories used in analysis were based on the two components of the 22 far-filed (measured 10 km or more from fault rupture) NGA PEER records[4)]. These 44 records have been identified by ATC 63 for collapse evaluation analysis[5)]. The selected 22 records correspond to a relatively large sample of strong recorded motions that are consistent with the code and are structure-type and site-hazard independent[6)]. Figure 10 presents the acceleration response spectra for these records. The design MCE spectrum is shown as the dark solid line in the figure. For analysis, the 44 records were first normalized and then scaled. Normalization of the records was done to remove the record-to-record variation in intensity.

Program OpenSees was used to conduct the nonlinear analyses described in this paper[3).] Pertinent model properties are listed here

- Analytical models are two-dimensional
- Beam and column elements, are represented as one dimensional frame elements. The members are prismatic and linear.
- Material nonlinearity is represented by concentrated plastic hinges represented by RBS hinges placed at the center of the reduced section
- The damper element is represented by the refined model including the limit states.
  For collapse analysis, the normalized records are then scaled upward or downward to obtain data points for the nonlinear incremental dynamic analysis (IDA) simulations[7).]

6. One Story Moment Frame

The one-story frame is square in plan and measures 27.4 m on each side. It is 4 m tall (see Figure 11). The structure has one interior steel moment resisting frame on the perimeter of each side. One of such frames was selected for design and analysis. The frame was designed using the code provisions and special seismic requirements for special moment resisting frames. The code maximum period used to compute base shear (Tmax=cuTa) is 0.31 second[6).] This period is used for scaling of ground motions as recommended by ATC 63.

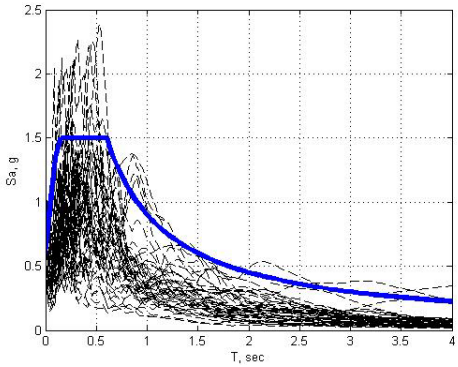

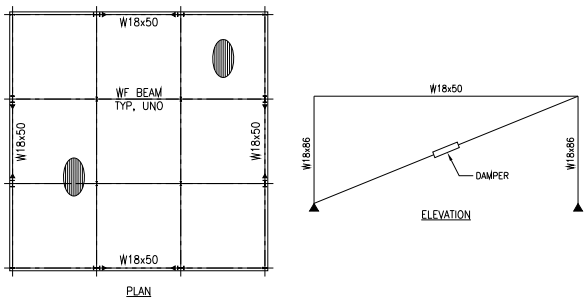

Fig.10: Response spectra of the records **Fig.11**: Views of one bay frame

6.1 Archetypes

Five one-story archetypes were analyzed. Details for these cases are listed in Table 1. For the remainder of this paper, result from cases O-2 and O-3 are presented.

Table 1: One story archetypes

Archetype→	O-1	O-2	O-3	O-4	O-5
Column base	Fixed	Pinned	Pinned	Fixed	Fixed
Dampers	No	Yes	Yes	Yes	Yes
Damper FS	Pinned	1.0 MCE	1.3 MCE	1.0 MCE	1.3 MCE

6.2 Pushover Analysis

Figure 12 presents the static pushover curve for archetypes O-2 and O-3. The pushover curves are asymmetric because the driver brace compression capacity exceeds piston undercut tensile capacity and because there is yield plateau for the buckling quadrant. Both systems are ductile with displacement ductility (μc) in excess of 8.00. The O-3 archetype is stronger because the damper has a higher factor of safety.

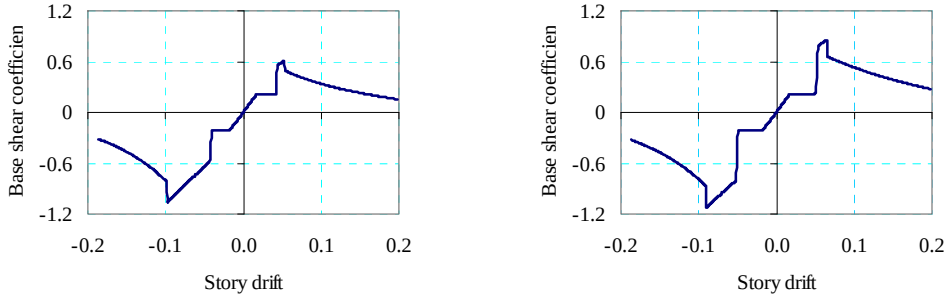

Fig.12: Pushover curves for archetypes O-2 and O-3

6.3 Incremental Dynamic Analysis (IDA)

Figure 13 presents the IDA plots for cases O-2 and O3. The data points and the analysis trends are identified by the dashed lines and markers. The plots are shown as the scaled input spectral acceleration (Sa) at period Tmax versus the story drift ratio.

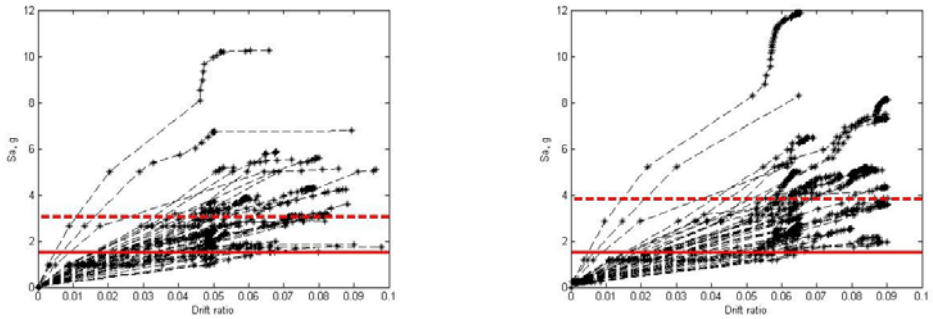

Fig.13: IDA curves for archetypes O-2 and O-3

The collapse point for each record was indented at the point where either the story drift ratio exceeded 0.18 or when the nonlinear tangent slope of the force-deformation curve dropped below 1% of the initial elastic slope. The median collapse Sa is (SCT) shown as the thick dashed line in the figures. The solid horizontal line is the Sa value at Tmax (SMT). The collapse margin ratio (CMR) is defined as the ratio of SCT and SMT. The adjusted collapse margin ratio (ACMR) is computed by multiplying the coefficient spectral shape factor (SSF) by the CMR. SSF depends on the building period and its ductility. Table 2 summarizes the pertinent data for the archetypes. Since the archetypes have ACMRs of greater than the ATC63 minimum (2.02), they both pass. However, the performance of archetype O-3 with a damper factor of safety is superior.

6.4 Fragility Plots

Figure 14 presents the fragility plots for cases O-2 and O3. The data points correspond to the 44 collapse Sa values. A best-fit log-normal plot is also shown in the figure. To account for uncertainties, ATC recommends a standard deviation (βTOT) of 0.55 for the case of good to excellent analysis method and available experimental data. Using this value, a revised fragility plot for each case was obtained. Using this plot, the probability of collapse at the MCE intensity is then computed. As shown in Table 2, both archetypes pass. However, the additional 30% factor of safety results in significant reduction in the collapse probability.

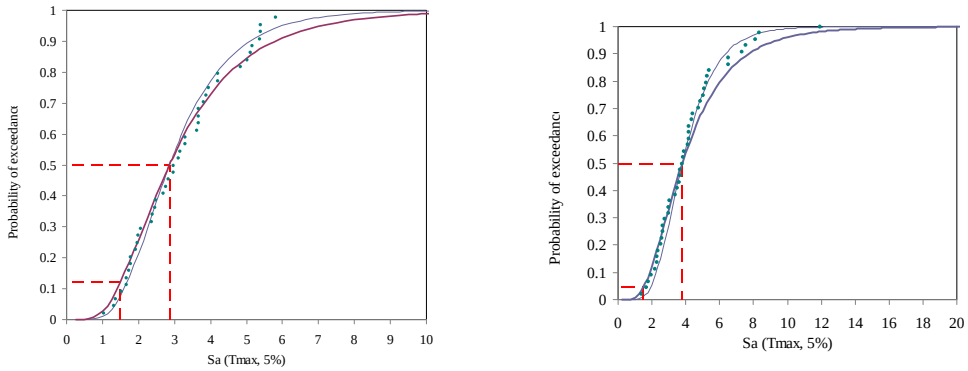

Fig.14: IDA curves for archetypes O-2 and O-3

Table 2: IDA results

Archetype	μc*	SSF	CMR	ACMR	$ACRM_{min}$	Pass/fail	MCE coll.	Max
O-2	8.00	1.34	2.02	2.70	2.02	Pass	15%	20%
O-3	8.00	1.34	2.54	3.39	2.02	Pass	5%	20%

7. Conclusions

Viscous dampers are added to steel moment frames structures can be used to reduce cost and improve seismic performance. IDA analysis was conducted to assess the efficacy of this methodology.

- For large earthquakes, the damper limit states must be accounted for.
- Structures designed per code provisions passed the ATC63 requirements.
- Addition of a factor of safety to the damper design is cost effective and improves the performance significantly.

Acknowledgements

Mr. Christopher Ariyaratana of University of Illinois was responsible for conducting the simulations reported in this paper. This effort is greatly appreciated. The authors acknowledge financial support from the Taylor Devices and Armor Steel. The technical assistance of Messrs. Doug Taylor and John Metzger of Taylor Devices and Dr. Kurt Haselton of California State University Chico is acknowledged.

References

1) Miyamoto, H.K. and Gilani, A., "Design of a new steel-framed building using ASCE 7 damper provisions", SEI institute ASCE Structures Congress. 2008. Vancouver, BC.
2) Pacific Earthquake Engineering Research Center, University of California, Berkeley, Open System for Earthquake Engineering Simulation (OpenSees), 2005. Berkeley, CA., USA
3) Taylor devices. Personal communications. 2008.
4) Pacific Earthquake Engineering Research Center, University of California, Berkeley, PEER NGA Records. 2007. Berkeley, CA., USA.
5) Federal Emergency Management Agency, "ATC 63, FEMA P695: Quantification of Building Seismic Performance Factors", 2007, Washington, D.C., USA.
6) American Society of Civil Engineers, "ASCE 7-05: Minimum design load for buildings and other structures", 2005, Reston, VA, USA.
7) Vamvatsikos, D. and Cornell, A.C., "Applied Incremental Dynamic Analysis", Earthquake Spectra, Volume 20, No. 2, pp. 523–553, 2004, Earthquake Engineering Research Institute, Oakland, CA, USA.